의학석사 학위논문

Comparison of conventional polychromatic and virtual monochromatic CT images in pediatric CT angiography: a phantom study to investigate the radiation dose saving effect

소아 전산화 단층촬영 혈관 조영술에서 고식적 다색 전산화 단층촬영 영상과 가상 단색 영상의 방사선량 절감 정도에 대한 비교 팬텀 연구

2018년 2월

서울대학교 대학원

의학과 영상의학 전공

최 형 인

Comparison of conventional polychromatic and virtual monochromatic CT images in pediatric CT angiography: a phantom study to investigate the radiation dose saving effect

지도 교수 김 우 선

이 논문을 의학석사 학위논문으로 제출함

2017년 12월

서울대학교 대학원
의학과 영상의학 전공
최 형 인

최형인의 의학석사 학위논문을 인준함
2018년 1월

위 원 장 _____ (인)

부위원장 _____ (인)

위 원 _____ (인)

Abstract

Purpose

The purpose of this phantom study was to investigate the radiation dose saving effect of virtual monochromatic images in dual-source dual-energy CT and low kilovoltage peak (kVp) polychromatic images in pediatric CT angiography when a 'noise constraint' was considered.

Materials and Methods

CT scans were performed at the second-generation dual-source 128-channel scanner, using two different-sized semi-anthropomorphic pediatric phantoms (ATOM model 704, 705; CIRS, Norfolk, VA) representing 1-year, and 5-year age-children, First, polychromatic images were obtained at five different levels of tube potential; 70 kV, 80 kV, 100 kV, 120 kV, and 140 kV using the same level of the automatic exposure control setting. Secondly, dual-energy CT scan using two different tube voltages (80 kVp and 140 kVp with tin filter) was performed and from DECT data, virtual monoenergetic image (VMI) sets were created from 40 to 100 keV at 10-keV increment using Mono and Mono+ image-based reconstruction algorithms, respectively. For each of nineteen (five conventional polychromatic images, seven Mono, and seven Mono+ reconstructed VMIs) image series for each phantom, CT attenuation numbers and standard deviations were measured by drawing circular regions of interest at the contrast insert and adjacent area of uniform tissue-equivalent attenuation. At each of five noise constraint levels (noise constraint=1.0, 1.1, 1.2, 1.5, 2.0), the relative dose factor (RDF) of each image set was calculated using 100 kVp polychromatic images as the reference.

Results

At the noise constraint of 1.1 and 1.2, the minimal RDF was observed at 80kVp polychromatic images for both phantom sizes (0.86 and 0.72 for the 1-year-old phantom and 0.88 and 0.74 for the 5-year-old phantom, respectively). At the noise constraint level of 1.5 and 2.0, 70kVp polychromatic images showed minimal RDF for both phantoms (0.52 and 0.47 for the 1-year-old phantom and 0.50 and 0.47 for the 5-year-old phantom, respectively). As for virtual monochromatic images, only Mono+ VMIs at 60keV revealed a dose-saving effect (RDF: 0.97) in the 1-year-old phantom, while the other levels of VMI showed no dose reduction effect (all RDFs >1).

Conclusion

For young children, 70 kVp polychromatic images are recommended for body CT angiography, if 50-100% of noise increase is tolerable. Low-voltage polychromatic images generally showed better dose saving potentials compared to virtual monochromatic images.

Keywords: Radiation dose, Virtual monochromatic image, Dual-source dual-energy CT, iodine Contrast-to-noise ratio with noise constraint

Student Number: 2016 - 21955

Contents

List of Tables

List of Figures

INTRODUCTION

Recently, the use of pediatric computed tomography (CT) has been rapidly increasing in diagnostic radiology [1, 2]. However, because of the potential for increased radiation exposure in children receiving these scans, pediatric CT screening should be performed appropriately. Pediatric patients should be more concerned about radiation exposure than adult population because children are more vulnerable to radiation than adults, have a longer life expectancy resulting in a larger window of opportunity for expressing radiation damage, and may receive a higher radiation dose than necessary if CT settings are not adjusted to their smaller body size [2]. Recent improvements in CT devices and reconstruction techniques have resulted in better image quality with lower doses.

Based on CT physics, as tube voltage gets close to the K-edge of iodine (33.2 kilo-electron volt, keV), the intrinsic attenuation of iodinated contrast media increases. Using low kilovoltage (kV) in CT angiography can increase vessel contrast and gain contrast-to-noise ratio (CNR) even with a slight inevitable increase in image noise. Therefore, using low kV in CT angiography can reduce radiation dose while maintaining CNR [3-5].

On the contrary to the conventional CT using single polychromatic tube voltage, dual-energy computed tomography (DECT) technique obtains data at two different tube voltage levels, which allows material composition analysis and reconstruction of monochromatic images at an arbitrary energy level [6]. Virtual monochromatic image reconstruction at different photon energy levels (keV) can lead to an improvement in iodine contrast in low-keV images and reduced metal artifacts in

high-keV images [7-11]. Especially in CT angiography, the use of low keV monochromatic images has advantages such as increased attenuation of iodine-containing arteries and consequently increased visibility of the arteries.

Recently a new monochromatic reconstruction algorithm was introduced to overcome rapid noise increase at low energy level of conventional monoenergetic reconstruction algorithms. Previous studies showed that this newly introduced advanced monoenergetic reconstruction (Mono+) improves image quality when compared with the conventional monoenergetic reconstruction (Mono) algorithm [12, 13]. These monochromatic images obtained by dual energy CT have been reported to have similar or superior diagnostic performance in various body part of CT angiography compared to conventional polychromatic CT [9, 14-17]. Regarding radiation dose, several previous studies insisted the dual energy CT images are dose-neutral or even shows dose reduction effect compared to the conventional polychromatic CT. However, there is not much research on how much radiation dose benefits can be expected with dual energy CT techniques compared to conventional polychromatic CT [18].

Even though we often use CNR as an image quality index when comparing image quality of CT images, noise constraint is needed because increased contrast does not necessarily guarantee improved image quality due to radical increase of absolute noise level that is clinically intolerable [19]. Yu et al. [19] proposed a new optimization index, called “iodine CNR with a noise constraint (iCNR_NC)” that limits the affordable image noise requirements.

To our knowledge, there is no study directly comparing low-kilovoltage peak (kVp) polychromatic images and virtual monoenergetic dual-energy CT images in terms of radiation dose. Therefore, the purpose of this phantom study was to

investigate the effect of virtual monochromatic images in dual-source dual-energy CT and low kilovoltage peak (kVp) polychromatic images on image quality and radiation dose in pediatric CT angiography when a ‘noise constraint’ was considered in addition to maintaining CNR.

MATERIALS AND METHODS

Phantom preparation

Two different-sized semi-anthropomorphic pediatric phantoms (ATOM model 704, 705; CIRS, Norfolk, VA) representing 1-year, and 5-year age-children were used in this study.

The height and weight were 75 cm/10 kg, and 110cm/19kg, respectively. The anteroposterior and lateral diameters at the thoracic level were 12 x 14 cm, and 14 x 17cm, respectively. The phantoms have 28 slices with slice thickness of 1.5 cm, or 26 slices with slice thickness of 2.5cm, respectively and it consists of materials of four different densities to represent four different tissues (bone, soft tissue, brain tissue, and lung tissue). These phantoms contain 168 or 180 removable plugs of 5-mm diameter to place samples or dosimeters at specific locations within organs (Fig. 1).

Two contrast rods containing two different iodine concentrations, 3.5 and 7.0 mg/ml of diluted nonionic contrast media (Iobitridol (Xenetix®) 350 mg/ml, Guerbet, Bloomington, USA) were placed in the central region of the phantoms to represent abdominal aorta in order to allow measurements of iodine-containing vessels and surrounding soft tissue of background tissue equivalent materials.

CT scan acquisition

All CT scans were performed with the second-generation dual-source 128-channel

scanner (SOMATOM Definition Flash; Siemens Healthcare, Forchheim, Germany)

First, polychromatic CT scanning was performed for each phantom at the following five available tube potential levels: 70 kV, 80 kV, 100 kV, 120 kV, and 140 kV using the automatic exposure control (AEC; CAREDose4D). The AEC setting was fixed at the quality reference mAs value of 150 and reference kV value of 120. This scanning protocol is currently used in our institute's daily CT practice. Usage of CAREDose4D provided real-time radiation dose reduction adjusting to the patient's size and shape [20]. Scanning parameters were as follows: rotation time, 0.28 s; pitch, 0.6; collimation, 64 x 0.6 mm; image thickness, 3.0 mm; slice interval, 2.0 mm. In the experimental design, a pitch of 0.6 was used to eliminate the mA limits at 70 kV. All images were reconstructed with dedicated iterative reconstruction (SAFIRE^{TM} [sonogram-affirmed iterative reconstruction], Siemens Health care) using a strength level of 3.

Secondarily, we performed dual-energy CT scan with the same machine using two X-ray tubes of two different tube voltages (80 kVp and 140 kVp, tin filter). Reference tube current-time product for 80 kVp tube was 200 mAs, and 77 mAs for Sn140 kVp tube. Using DECT data, virtual monoenergetic image (VMI) sets were created from 40 to 100 keV at 10-keV increments using both Mono and Mono+ image-based reconstruction algorithms, resulting in 7 image sets for each algorithm. Although the DECT used for this study could be reconstructed with monoenergetic images above 100 keV, we did not perform imaging at higher keV levels because the iodine attenuation was expected to be too faint [21].

It was not necessary to match CTDI for the purpose of calculations because only relative dose, i.e. relative dose factor (RDF), was considered and the absolute CTDI is irrelevant for the purpose of calculating RDF [19].

CT Image Analysis

For each of nineteen (five conventional polychromatic images, seven Mono, and seven Mono+ reconstructed VMI) contiguous image series of each phantom scan, we measured the CT attenuation numbers and standard deviation in the region of interests. One circular ROI was placed in the center of the contrast insert (ROI_{in}) and another ROI (ROI_{out}) was placed 1.0 or 2.0 cm above the contrast insert in the 1-year-old and 5-year-old phantom, respectively, in an area of uniform tissue-equivalent attenuation area. Each ROI_{in} was maximized within the contrast insert area while excluding surrounding tissue-equivalent area (11.80 mm^2 for 1-year-old phantom; 104.62 mm^2 in 5-year-old phantom) (Fig. 2). A contrast-to-noise ratio (CNR) was calculated for each image dataset as the difference in mean HU between ROI_{in} and ROI_{out} divided by noise (σ) defined as the standard deviation of HU for ROI_{out} [17, 22]. The measurements of each series of images were measured three times and averaged each to reduce the measured variability.

iCNR_NC include an additional variable that allows adjustment of image noise requirements, which are set according to the clinical need:

$$CNR_{kV} \geq CNR_{kV\text{-}ref},$$

$$\sigma_{kV} \leq \alpha \cdot \sigma_{kV\text{-}ref},$$

where α can be adjusted to allow varying conditions of noise as at the reference tube potential. From the concept of iCNR_NC, we can calculate the RDF for each kV compared to the reference kV with the predefined noise constraint parameter (α); e. g. noise constraint=1.0, 1.1, 1.2, 1.5, 2.0. The RDF is given by

$$\text{RDF} = \max\left[\left(\frac{C_{kV-ref}}{C_{kV}}\right)^2, \frac{1}{\alpha^2}\right] \cdot \frac{\sigma_{kV}{}^2}{\sigma_{kV-ref}{}^2} \ .$$

The RDF can be used to quantify the relative dose of a tube potential for a given CNR of a particular contrast material. For example, for a reference tube potential of 100 kV, a RDF of 1.2 at 120 kV means that 120 kV requires 20% higher radiation dose to meet the same image quality as 100 kV. A RDF of 0.6 at 80 kV means that 80 kV requires 40% less radiation dose to get the same image quality as 100 kV.

We used 100 kVp as the reference kV (kV_{ref}) in the relative dose factor calculation because it reflected the kV setting of our clinical CT angiography protocol prior to this study [23].

The RDF was calculated where noise constraint α can be adjusted to allow varying conditions of noise as at the reference tube potential. A noise constraint equal to 1.00 represent zero tolerance for noise increase and any noise increase is not permitted. A noise constraint of 1.1 indicates a 10% increase in noise tolerance and noise constraint values of 1.2, 1.5, and 2.0 indicate a 20%, 50% and 100% noise increase, respectively. The noise constraint parameter α can be applied to various clinical applications. For example, α =1 in the case of the non-contrast exams; α =1.1-1.25 for contrast-enhanced routine exams; and α =1.5-2.0 for CT angiography depending on how much noise a radiologist can afford [19].

The RDF is the contrast "ratio" to the reference kV, so it is not affected by changes in iodine concentration. We were able to average the contrast ratio across different iodine concentrations for each kV and phantom size. This reduced statistical complexity and allowed us to obtain a single relative dose factor for each kV, noise constraint and phantom size.

RESULTS

Contrast

Table 1 and Fig. 3 display the values for iodine contrast (C), noise (σ), and CNR for all kVp, keV settings for different phantom sizes at the contrast medium concentration of 7.0 mg/ml. As expected, the iodine contrast increased as tube potential decreased both in monochromatic and polychromatic energy. The iodine contrast at lower monoenergetic reconstruction level below 60 keV was higher than that at polychromatic images.

Noise

The noise values displayed in the Table 1 cannot be directly compared among difference polychromatic tube voltage levels because CTDI was not matched across kV settings even though the AEC setting was constant.

As for virtual monochromatic reconstruction, Mono, and Mono+ monochromatic images provided lowest noise level at 70-80 keV, with progress increment beyond the optimal energy level to 100 keV. This is consistent with previous studies about monochromatic images [14, 18]. At lower energy level, the noise in Mono images rapidly increased, however, Mono+ markedly decreased excessive noise thanks to advanced noise reduction technique. (Fig. 4) Also, the noise was generally lower using Mono+ compared to Mono at the same keV level. Such tendency was greater at the abdomen than at the chest in both 1-year-old and 5-year-old phantoms,

because the larger the body part, the more photon attenuates.

Relative dose factor (RDF)

Table 2 and Fig. 5 display the RDF for each polychromatic tube potential and monochromatic energy level for all phantom sizes and noise constraints. The noise constraint parameter was set to α=1.0, 1.1, 1.2, 1.5, 2.0, respectively. Reference kV was 100 kVp which is the most commonly used in daily CT angiography practice. At α=1.0, the desired image quality must satisfy two conditions: the CNR is not less than that obtained from the reference tube potential and the noise is not higher than that obtained from the reference tube potential. At α=1.5, the desired image quality should satisfy two conditions: CNR is not less than that obtained from the reference tube potential, and the noise is not higher than 1.5 times the noise obtained from the reference tube potential, i.e., up to 50% higher noise tolerance than 100 kVp.

At α=1.0, 100kVp polychromatic images showed the lowest RDF of 1.0 and all the other kV levels of image series showed the higher RDFs of more than 1.0. RDFs at 70 kVp were 1.17, and 1.13 for 1-year-old abdomen, and 5-year-old abdomen, respectively. This means that a 17%, and 13% increase in radiation dose is required to match the noise level with the 100 kVp polychromatic images.

At the noise constraint of 1.1 and 1.2, the minimal RDF was observed at 80kVp polychromatic images for both phantom sizes (0.86 and 0.72 for the 1-year-old phantom and 0.88 and 0.74 for the 5-year-old phantom, respectively). At the noise constraint level of 1.5 and 2.0, 70kVp polychromatic images showed minimal RDF for both phantoms (0.52 and 0.47 for the 1-year-old phantom and 0.50 and 0.47 for

the 5-year-old phantom, respectively).

At α=1.5, the RDFs of 70 kVp polychromatic images were 0.52, and 0.50 for 1-year-old abdomen, and 5-year-old abdomen, respectively. The radiation dose reduction could be achieved by 48%, and 50 %. In general, higher noise constraint was associated with lower RDF, which means greater radiation dose reduction potential. (Fig. 6)

As for virtual monochromatic images, the lowest RDF was obtained at 70 keV at α=1.0, 1.1, 1.2, 1.5, and 60 keV at α=2.0 in 1-year-old abdomen phantom. Similarly, 5-year-old abdomen phantom showed the lowest RDF at 70 keV for α=1.0, and 60 keV for α=1.1, 1.2, 1.5, 2.0. In the mono + reconstruction images, the lowest RDF was found at α=1.0 at 80 keV, α=1.1 and 1.2 at 70 keV, α=1.5 and 2.0 at 60 keV in 1-year-old abdomen phantom, and with α=1.0 at 70 keV, α=1.1, 1.2, 1.5 at 60 keV, α= 2.0 at 50 keV in 5-year-old abdomen phantom, respectively. However, when compared to the 100kVp polychromatic reference images, only Mono+ VMIs at 60 keV revealed a dose-saving effect (RDF: 0.97) in the 1-year-old phantom with α=2.0, while the other levels of VMIs showed no dose reduction effect (all RDFs >1).

Based on these RDF values shown in the table 2, one can easily select the most dose-efficient tube potential for each phantom size and body part when different noise constraints are applied. Table 3 shows optimal tube potential and the corresponding dose reduction for each phantom size, and different noise constraints. All phantom sizes reached a minimum RDF at 70 kV with noise constraint 1.5 and 2.0. The optimal tube potential and different noise constraints should be selected to best suit different clinical settings.

DISCUSSION

There have been few studies comparing the radiation dose and image quality of virtual monoenergetic images produced with dual-energy dual-source CT and conventional polychromatic images systemically in various-sized pediatric patients.

Iodine contrast was much higher at monoenergetic reconstruction energy level between 40 and 60 keV than the 100 kVp conventional polychromatic images, but the image noise was also higher at lower monoenergetic reconstruction level, especially in Mono algorithm. The Mono 40 keV reconstruction images showed more than four times as much noise as 100 kVp polychromatic images. (38.11, and 7.59 in 5-year-old abdomen scan, respectively)

Monochromatic images reconstructed by advanced or conventional technique seldom showed radiation dose reduction compared to reference polychromatic CT (100 kVp), except for Mono+ at 60 keV with noise constraint 2.0 in 1-year-old phantom. This means that there is a dose penalty (RDF > 1.0) in both mono and mono+ images for all phantom sizes and noise constraints except for 1-year-old abdomen with Mono+ 60 keV (α=2.0, RDF=0.97). This is caused by relatively higher noise level of low-kV VMIs compared to reference conventional polychromatic (100 kVp) images. Only with highest noise constraint α=2.0, optimal Mono+ images achieved dose gain by 3% in 1-year-old phantom, however these values were inferior to those achieved by 70 or 80 kVp conventional polychromatic images. Therefore, any energy level of monochromatic reconstruction is not suitable for pediatric CT angiography in terms of radiation dose. The term ‘dose penalty’ is intended to reflect the necessity for dose increase

to maintain the diagnostic value of the study as quantified by the 'iCNR_NC'. If only CNR was used as the quality measure, there would be no such dose penalty; however, this poses the risk of non-diagnostic exams due to excessive noise.

Using 70 kV does allow for radiation dose reduction in both 1-year-old and 5-year-old phantom with a noise constraint of 1.5. (48%, 50% dose reduction for 1-year-old, 5-year-old scan, respectively). However, this should be made in the clinical context that the radiologist must be willing to accept a higher level of image noise as a trade-off to increased vessel contrast. This absolute increase in noise is very subtle (3.80 HU ($\alpha = 1.5$)) and would not have a significant impact on the radiologist.

There are several limitations to our study. First, we used only two different-sized phantoms, which are 1-year-old equivalent, and 5-year-old equivalent. We chose phantom study instead of actual patients' study because it is unethical to scan children several times for experimental purpose. However, we can overcome this limitation because the phantoms of our study mimic the attenuation characteristics of actual patients. We omit phantoms equivalent to newborn and to patients over 10 years of age. The phantom sizes in our study are much smaller than the phantom sizes used by Yu et al. [19]. For the relatively small phantom sizes used here, the effect of kV on noise for a matched CTDI is much less than the effect in the larger phantoms. For the same reason, CNR difference between different contrast medium concentrations was not significant. Additional studies on phantom of various sizes are need. Second, the single pitch factor of 0.6 for our CT protocol should be in consideration. We chose this low pitch value to avoid potential limitation in generating tube current at low kV imaging, which was also used by the other studies of Yu et al. [19], and MacDougall et al. [24]; however, in practice, the

scanning time and motion artifact are also factors to consider when imaging people especially pediatric patients. Third, iCNR_NC is a reasonable image quality metric that considers iodine contrast and noise at the same time, but does not reflect the beam-hardening effect or electronic noise that also affect image quality. Especially beam-hardening effect can be more problematic in low kV, such as 70 kVp selected in our study. Fourth, we finally recommended 70 kVp with noise constraint 1.5 or 2.0. For contrast-enhanced CT angiography, a visibility of the iodine-enhanced vascular structures is of primary interest. Since the vessel's iodine contrast is higher at lower kV, relatively higher noise can be tolerated. That is, a relatively high noise constraint of 1.5 to 2.0 could be used at the discretion of the reading radiologist. For contrast-enhanced routine chest or abdomen CT, however, soft tissue areas with less iodine uptake are also of diagnostic interest. Therefore, iodine CNR alone is not appropriate for diagnostic task, i.e. too high noise level cannot be affordable, and a relatively strict noise constraint should be applied. The optimal noise constraint value for each clinical exam should be carefully evaluated. The generalized image quality index, iCNR_NC, can take a role in determining various daily CT protocols. At last, further studies are needed to track the real value of radiation dose reduction by imaging actual patients with the CT protocol proposed in our study (taken at 70 kVp on CT angiography). Specialized radiologists and technicians can select proper noise constraint based on individual patient and each diagnostic task.

CONCLUSION

For young children, 70 kVp polychromatic images are recommended for body CT angiography, if 50-100% of noise increase is tolerable. Low-voltage polychromatic images generally showed better dose saving potentials compared to virtual monochromatic images.

REFERENCES

1. Zacharias C, Alessio AM, Otto RK, et al (2013) Pediatric CT: Strategies to Lower Radiation Dose. American Journal of Roentgenology 200:950-956.

2. Almohiy H (2014) Paediatric computed tomography radiation dose: A review of the global dilemma. World Journal of Radiology 6:1-6.

3. Gnannt R, Winklehner A, Goetti R, et al (2012) Low kilovoltage CT of the neck with 70 kVp: comparison with a standard protocol. AJNR American journal of neuroradiology 33:1014-1019.

4. Schindera ST, Graca P, Patak MA, et al (2009) Thoracoabdominal-aortoiliac multidetector-row CT angiography at 80 and 100 kVp: assessment of image quality and radiation dose. Investigative radiology 44:650-655.

5. Wintersperger B, Jakobs T, Herzog P, et al (2005) Aorto-iliac multidetector-row CT angiography with low kV settings: improved vessel enhancement and simultaneous reduction of radiation dose. European radiology 15:334-341.

6. Yu L, Leng S, McCollough CH (2012) Dual-Energy CT–Based Monochromatic Imaging. American Journal of Roentgenology 199:S9-S15.

7. Bamberg F, Dierks A, Nikolaou K, et al (2011) Metal artifact reduction by dual energy computed tomography using monoenergetic extrapolation. European radiology 21:1424-1429.

8. Yu L, Christner JA, Leng S, et al (2011) Virtual monochromatic imaging in dual-source dual-energy CT: radiation dose and image quality. Medical physics 38:6371-6379.

9. Apfaltrer P, Sudarski S, Schneider D, et al (2014) Value of monoenergetic low-kV dual energy CT datasets for improved image quality of CT pulmonary

angiography. Eur J Radiol 83:322-328.

10. Marin D, Boll DT, Mileto A, et al (2014) State of the art: dual-energy CT of the abdomen. Radiology 271:327-342.

11. Schneider D, Apfaltrer P, Sudarski S, et al (2014) Optimization of kiloelectron volt settings in cerebral and cervical dual-energy CT angiography determined with virtual monoenergetic imaging. Academic radiology 21:431-436.

12. Meier A, Wurnig M, Desbiolles L, et al (2015) Advanced virtual monoenergetic images: improving the contrast of dual-energy CT pulmonary angiography. Clinical radiology 70:1244-1251.

13. Albrecht MH, Scholtz JE, Husers K, et al (2016) Advanced image-based virtual monoenergetic dual-energy CT angiography of the abdomen: optimization of kiloelectron volt settings to improve image contrast. European radiology 26:1863-1870.

14. Kang M-J, Park CM, Lee C-H, et al (2010) Dual-Energy CT: Clinical Applications in Various Pulmonary Diseases. RadioGraphics 30:685-698.

15. Zhang L-J, Wu S-Y, Niu J-B, et al (2010) Dual-Energy CT Angiography in the Evaluation of Intracranial Aneurysms: Image Quality, Radiation Dose, and Comparison With 3D Rotational Digital Subtraction Angiography. American Journal of Roentgenology 194:23-30.

16. Vlahos I, Chung R, Nair A, et al (2012) Dual-Energy CT: Vascular Applications. American Journal of Roentgenology 199:S87-S97.

17. Sudarski S, Apfaltrer P, Nance JW, Jr., et al (2013) Optimization of keV-settings in abdominal and lower extremity dual-source dual-energy CT angiography determined with virtual monoenergetic imaging. Eur J Radiol 82:e574-581.

18. Henzler T, Fink C, Schoenberg SO, et al (2012) Dual-Energy CT: Radiation Dose Aspects. American Journal of Roentgenology 199:S16-S25.
19. Yu L, Li H, Fletcher JG, et al (2010) Automatic selection of tube potential for radiation dose reduction in CT: a general strategy. Medical physics 37:234-243.
20. Mayer C, Meyer M, Fink C, et al (2014) Potential for Radiation Dose Savings in Abdominal and Chest CT Using Automatic Tube Voltage Selection in Combination With Automatic Tube Current Modulation. American Journal of Roentgenology 203:292-299.
21. Grant KL, Flohr TG, Krauss B, et al (2014) Assessment of an advanced image-based technique to calculate virtual monoenergetic computed tomographic images from a dual-energy examination to improve contrast-to-noise ratio in examinations using iodinated contrast media. Investigative radiology 49:586-592.
22. Szucs-Farkas Z, Strautz T, Patak MA, et al (2009) Is body weight the most appropriate criterion to select patients eligible for low-dose pulmonary CT angiography? Analysis of objective and subjective image quality at 80 kVp in 100 patients. European radiology 19:1914-1922.
23. Yu L, Liu X, Leng S, et al (2009) Radiation dose reduction in computed tomography: techniques and future perspective. Imaging in medicine 1:65-84.
24. MacDougall RD, Kleinman PL, Yu L, et al (2016) Pediatric thoracic CT angiography at 70 kV: a phantom study to investigate the effects on image quality and radiation dose. Pediatric radiology 46:1114-1119.

Table 1 Iodine contrast, noise, and CNR for all kVp, keV settings for different phantom sizes with contrast medium concentration 7.0 mg/ml

Phantom	Energy Level	$Contrast_{in}$ (HU)	$Contrast_{out}$ (HU)	Noise (HU)	CNR
1-year-old	*Polychromatic*				
	70 kVp	456.25	21.73	7.24	60.02
	80 kVp	389.60	22.51	6.88	53.36
	100 kVp	299.12	25.43	6.79	40.31
	120 kVp	239.57	26.59	6.07	35.09
	140 kVp	203.52	26.05	7.22	24.58
	Monochromatic (Mono)				
	40 keV	747.07	8.82	35.39	20.86
	50 keV	487.89	18.11	19.77	23.76
	60 keV	330.15	23.76	11.71	26.16
	70 keV	232.86	27.27	9.15	22.47
	80 keV	170.62	29.52	9.53	14.81
	90 keV	129.08	30.99	10.66	9.20
	100 keV	100.40	32.05	11.78	5.80
	Monochromatic (Mono+)				
	40 keV	719.43	11.37	19.96	35.47
	50 keV	475.49	18.95	14.43	31.64
	60 keV	327.11	23.58	11.08	27.39
	70 keV	232.71	26.42	9.08	22.72
	80 keV	170.39	28.40	7.75	18.32
	90 keV	129.04	29.78	7.3	13.60
	100 keV	100.53	30.74	7.04	9.91
5-year-old	*Polychromatic*				
	70 kVp	422.14	19.27	8.17	49.31
	80 kVp	354.12	24.55	7.81	42.20
	100 kVp	271.06	27.60	7.59	32.08
	120 kVp	219.41	29.05	8.33	22.85
	140 kVp	186.92	29.21	8.98	17.56

	Monochromatic (Mono)				
	40 keV	710.52	11.05	38.11	18.36
	50 keV	472.10	18.23	21.52	21.11
	60 keV	324.25	24.62	11.15	27.00
	70 keV	233.73	26.87	9.33	22.25
	80 keV	175.46	29.36	10.87	13.53
	90 keV	138.16	30.47	13.04	8.28
	100 keV	111.56	31.20	13.94	5.74
	Monochromatic (Mono+)				
	40 keV	709.26	8.50	20.41	34.35
	50 keV	469.13	17.23	13.52	33.49
	60 keV	321.91	21.88	10.33	29.14
	70 keV	232.60	26.86	8.82	23.39
	80 keV	174.82	28.75	8.23	17.82
	90 keV	136.71	30.51	8.97	11.93
	100 keV	110.20	31.59	9.25	8.55

Table 2 Relative dose factor for phantom sizes, noise constraints, and kilovoltage (kV), reconstruction algorithm and energy level (keV) settings relative to the 100-kVp reference setting

Phantom	Energy Level	Relative Dose Factor				
		Noise Constraints (α)				
		1.0	**1.1**	**1.2**	**1.5**	**2.0**
1-year-old	*Polychromatic*					
	70 kV	1.17	0.97	0.81	**0.52***	**0.47***
	80 kV	1.04	**0.86***	**0.72***	0.63	0.63
	100 kV	**1.00***	1.00	1.00	1.00	1.00
	120 kV	1.24	1.24	1.24	1.24	1.24
	140 kV	2.53	2.53	2.53	2.53	2.53
	Monochromatic (Mono)					
	40 keV	28.26	23.36	19.63	12.56	7.07
	50 keV	8.82	7.29	6.13	3.92	2.21
	60 keV	3.09	2.56	2.15	1.38	**1.06**†
	70 keV	**1.89**†	**1.56**†	**1.31**†	**1.31**†	1.31
	80 keV	2.64	2.64	2.64	2.64	2.64
	90 keV	5.76	5.76	5.76	5.76	5.76
	100 keV	11.64	11.64	11.64	11.64	11.64
	Monochromatic (Mono+)					
	40 keV	8.99	7.43	6.24	4.00	2.25
	50 keV	4.70	3.88	3.26	2.09	1.18
	60 keV	2.77	2.29	1.92	**1.23**§	**0.97**§
	70 keV	1.86	**1.54**§	**1.29**§	1.29	1.29
	80 keV	**1.75**§	1.75	1.75	1.75	1.75
	90 keV	2.71	2.71	2.71	2.71	2.71
	100 keV	4.15	4.15	4.15	4.15	4.15

5-year-old	*Polychromatic*					
	70 kV	1.13	0.93	0.78	**0.50***	**0.47***
	80 kV	1.06	**0.88***	**0.74***	0.62	0.62
	100 kV	**1.00***	1.00	1.00	1.00	1.00
	120 kV	1.83	1.83	1.83	1.83	1.83
	140 kV	2.82	2.82	2.82	2.82	2.82
	Monochromatic (Mono)					
	40 keV	24.35	20.12	16.91	10.82	6.09
	50 keV	7.75	6.41	5.38	3.45	2.56
	60 keV	2.07	**1.71**†	**1.45**†	**1.45**†	**1.45**†
	70 keV	**1.95**†	1.95	1.95	1.95	1.95
	80 keV	4.67	4.67	4.67	4.67	4.67
	90 keV	10.94	10.94	10.94	10.94	10.94
	100 keV	19.32	19.32	19.32	19.32	19.32
	Monochromatic (Mono+)					
	40 keV	6.98	5.77	4.85	3.10	1.75
	50 keV	3.06	2.53	2.12	1.36	1.02
	60 keV	1.78	**1.47**§	**1.26**§	**1.26**§	**1.26**§
	70 keV	**1.76**§	1.76	1.76	1.76	1.76
	80 keV	2.71	2.71	2.71	2.71	2.71
	90 keV	5.22	5.22	5.22	5.22	5.22
	100 keV	8.59	8.59	8.59	8.59	8.59

* Minimal RDF among all images with same phantom size, noise constraints

† Minimal RDF among Mono reconstruction images with same noise constraints

§ Minimal RDF among Mono+ reconstruction images with same noise constraints

Table 3 Optimal kV and dose reduction percentage in different phantom sizes

1-year-old phantom			5-year-old phantom		
α	Optimal kV	Dose Reduction (%)	**α**	Optimal kV	Dose Reduction (%)
1.0	100	-	**1.0**	100	-
1.1	80	14	**1.1**	80	12
1.2	80	28	**1.2**	80	26
1.5	70	48	**1.5**	70	50
2.0	70	53	**2.0**	70	53

α : Noise Constraints

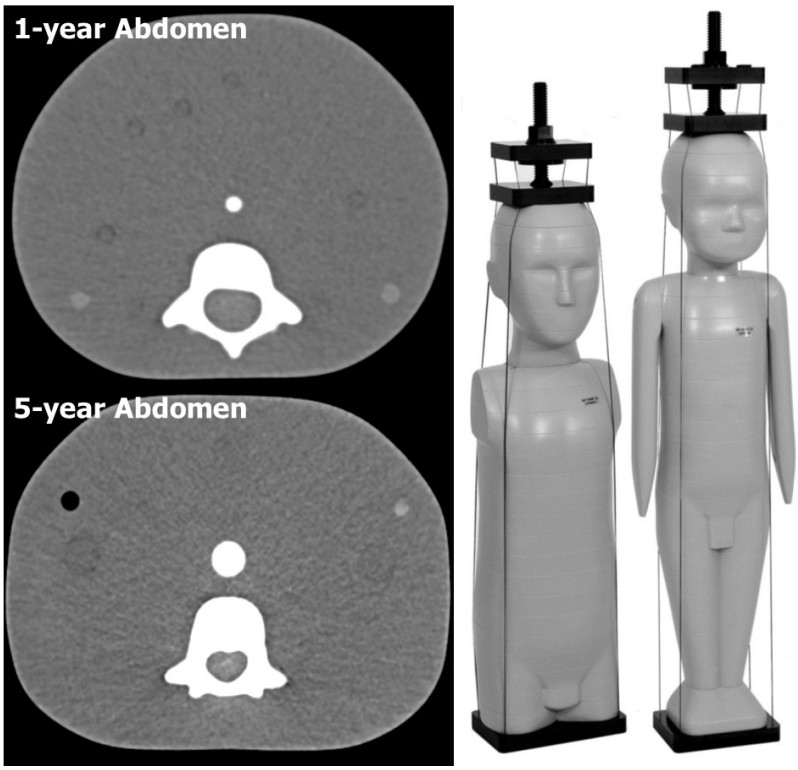

Fig. 1 A semi-anthropomorphic pediatric abdominal phantoms and transaxial CT images. Iodine contrast rod were placed in the center of the phantom. The anteroposterior and lateral thoracic diameters were 12x14 cm, and 14x17 cm for 1-year and 5-year-old phantom, respectively.

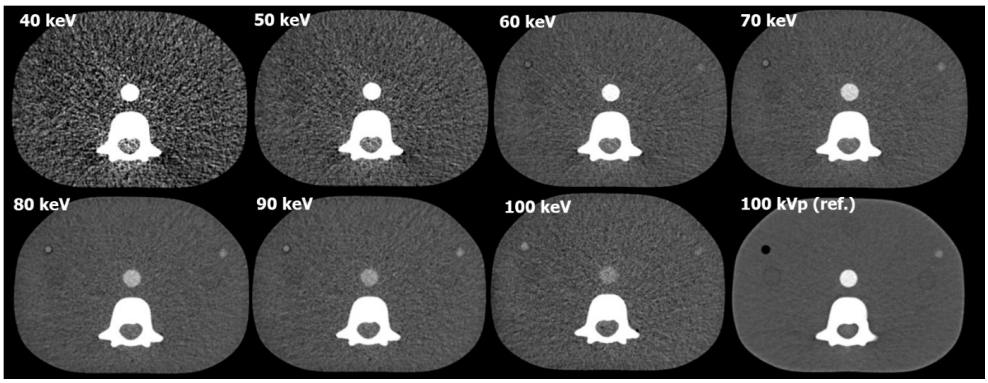

Fig. 2 An example of virtual monochromatic image (Mono) sets from 40 keV to 100 keV created from a dual-energy scan and reference image from polychromatic 100 kVp scan (Window width 400 HU, level 100 HU). As the keV decreases, iodine contrast attenuation increases, but the noise was also increases. VMI at 40 keV shows excessive image noise.

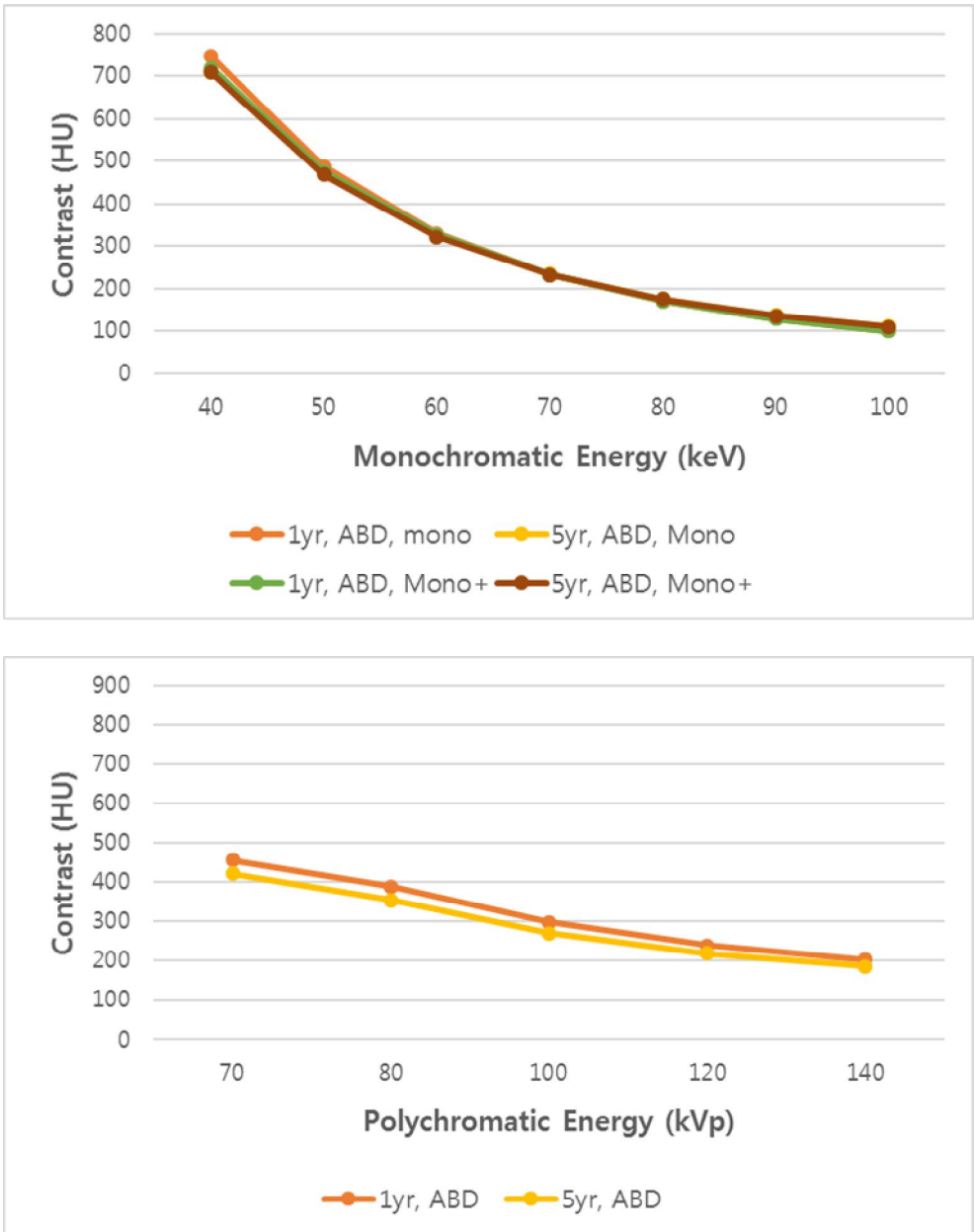

Fig. 3 (a) Iodine contrast as a function of monochromatic energy for the different phantom sizes. For comparison, iodine contrasts at different polychromatic energies are also displayed in (b). The iodine contrast is relatively consistent depending on the kVp of the polychromatic image or the keV of the monochromatic image regardless of the size or body part.

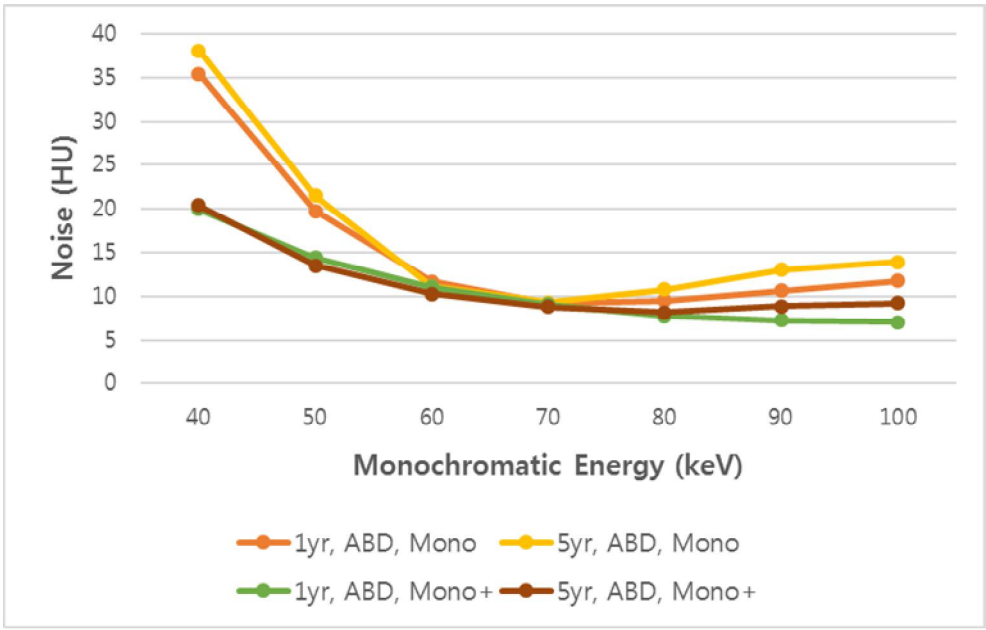

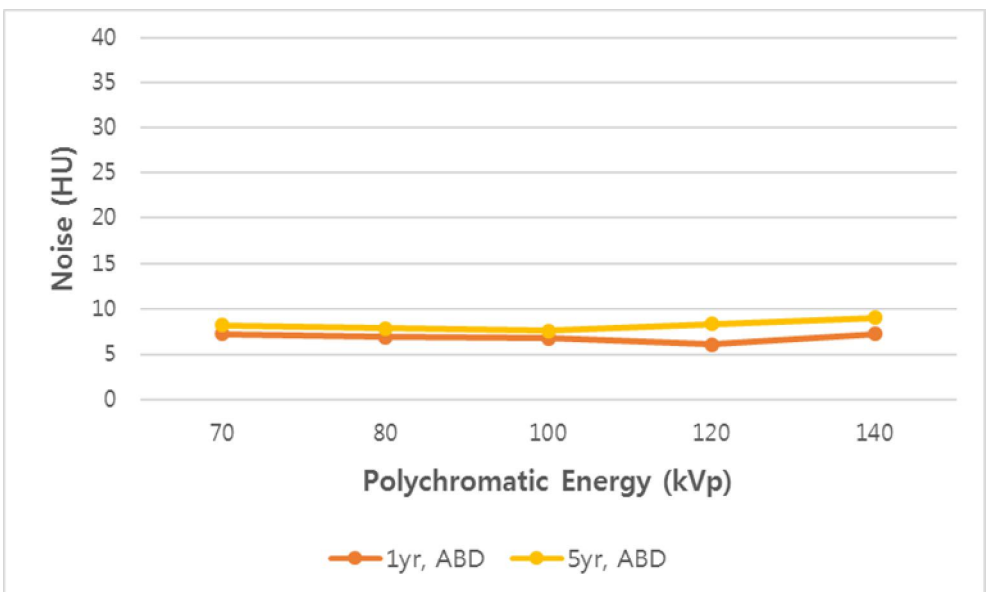

Fig. 4 (a) Noise as a function of monochromatic energy for the different phantom sizes. For comparison, noises at different polychromatic energies are also displayed in (b). Although the radiation doses in terms of CTDI are not matched between different sizes and body parts, we can see that the 70-80 keV VMI tends to exhibit minimal noise, which is comparable to the noise of polychromatic energy.

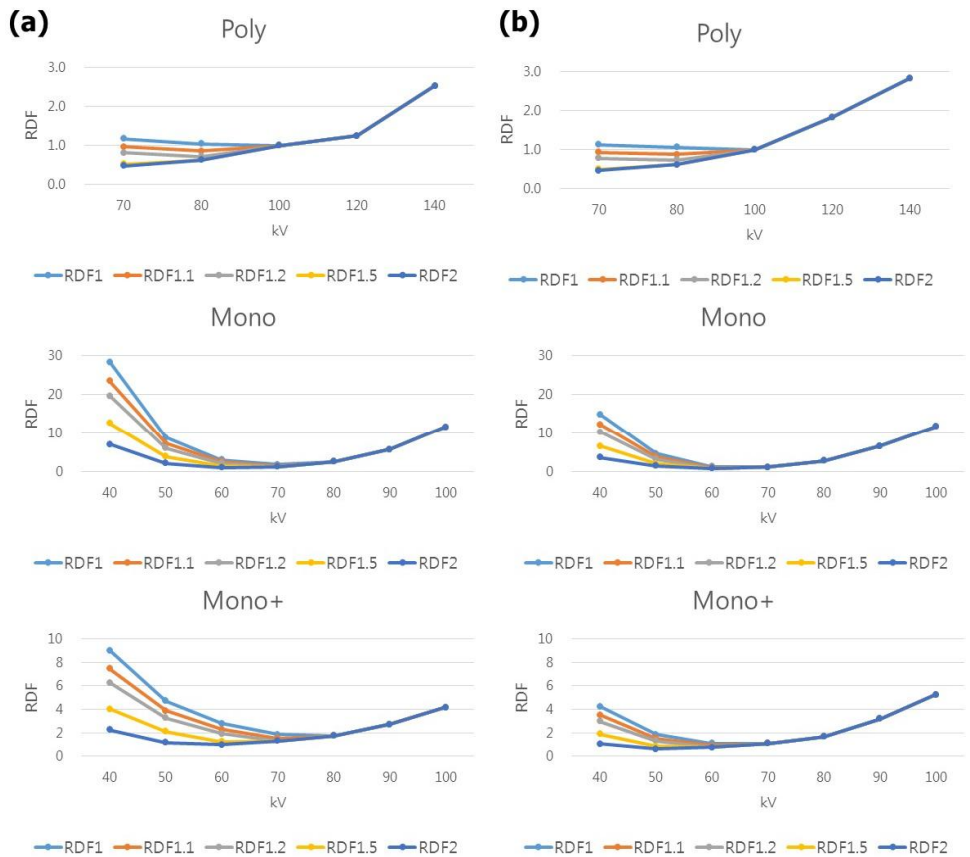

Fig. 5 Relative dose factor (RDF) at all different energy level both for conventional polychromatic CT and virtual monochromatic images with the different noise constraints at (a) 1-year-old abdomen, (b) 5-year-old abdomen phantom, respectively.

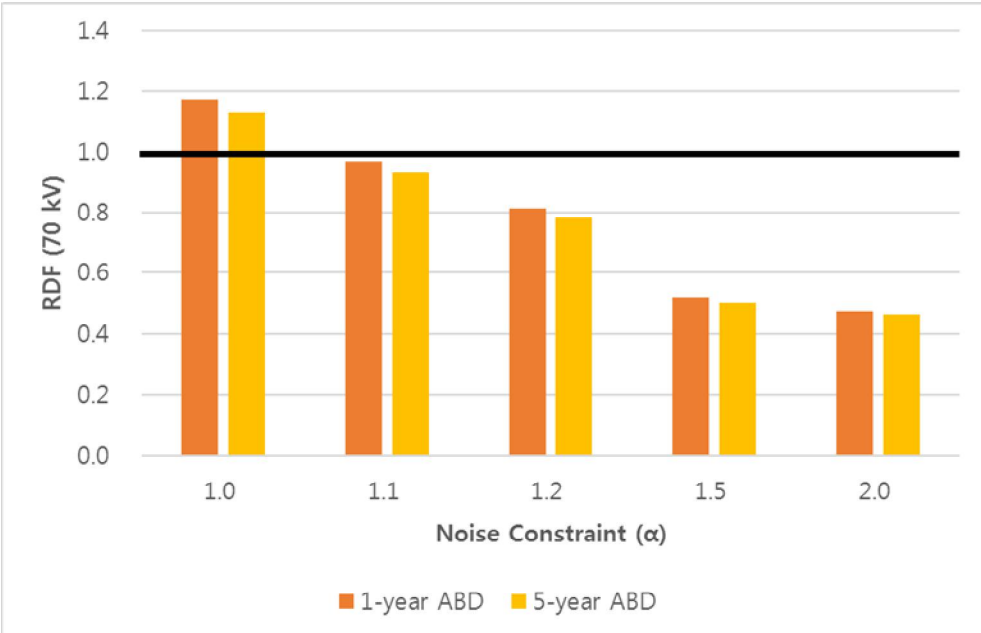

Fig. 6 Relative dose factor (RDF) at 70 kVp for the different phantom sizes and five noise constraints.

국문 초록

소아 전산화 단층촬영 혈관 조영술에서 고식적 다색 전산화 단층촬영 영상과 가상 단색 영상의 방사선량 절감 정도에 대한 비교 팬텀 연구

목적

이 팬텀 연구의 목적은 '잡음 제한'을 고려했을 때 소아 전산화 단층촬영 혈관 조영술에서 저 관전압 다색 전산화 단층촬영 영상 및 이중선원 이중에너지 전산화 단층촬영을 이용한 가상 단색 영상의 방사선량 절감 효과를 조사하는 것이다.

재료 및 방법

이번 연구의 모든 전산화 단층 촬영은 2세대 이중선원 128채널 촬영 장치를 이용하여 수행되었으며, 1세 또는 5세를 대표하는 두 가지 크기의 반-의인화 소아 팬텀 (ATOM 모델 704, 705, CIRS, Norfolk, VA)을 사용했다. 우선, 70 kV, 80 kV, 100 kV, 120 kV 및 140 kV의 다섯 가지의 관전압에서 다색 전산화 단층촬영 영상을 촬영하였다. 둘째, 두 개의 서로 다른 튜브 전압 (80 kVp와 140 kVp)을 사용하는 이중 에너지 전산화 단층촬영을 수행하였고, 이로 얻은 영상 자료를 이용하여 40 keV에서 100 keV까지 10 keV 단위로 가상 단색 영상을 Mono 및 Mono + 재구성 알고리즘을 사용하여 만들었다. 각 팬텀에 대해 얻어진 19 개의 영상 (5 개의 고식적 다색 영상, 각 7 개의 Mono 및 Mono + 단색 영상)에서 관심영역을 그려 전산화 단층촬영 감쇠계수 및 표준 편차를 구했다. 5 개의 잡음 제한 계수 (잡음 제약 = 1.0, 1.1, 1.2, 1.5,

2.0)에 대해, 100 kVp 다색 이미지를 기준으로 한 각 영상의 상대 선량 계수를 계산하였다.

결과

잡음 제한이 1.1, 또는 1.2일 경우, 최소 상대 선량 계수는 80 kVp 다색 영상에서 얻어졌으며, 각각 1세 팬텀에서 0.86과 0.72, 5세 팬텀에서 0.88과 0.74로 측정되었다. 잡음 제한이 1.5, 또는 2.0일 경우, 최소 상대 선량 계수는 70 kVp 다색 영상에서 얻어졌으며, 각각 1세 팬텀에서 0.52와 0.47, 5세 팬텀에서 0.50과 0.47로 측정되었다. 가상 단색 영상의 경우, 60 keV의 Mono+ 재구성 기법으로 만들어진 1세 팬텀 영상에서만 방사선량 감소 효과 (상대 선량 계수: 0.97)를 보였고, 다른 가상 단색 영상은 선량 감소 효과가 없었다. (모든 상대 선량 계수> 1).

결론

소아 전산화 단층촬영 혈관 조영술에서 50-100%의 영상 잡음 증가를 허용한다면 70 kVp 다색 전산화 단층촬영 영상을 권장한다. 고식적 저관전압 다색 영상은 대체로 가상 단색 영상에 비해 방사선량 절감 정도에 있어서 우월하다.

주요어 : 소아, 방사선량, 가상 단색 영상, 이중선원 이중에너지 전산화 단층 촬영
학 번 : 2016 - 21955